IARJSET ISSN (O) 2393-8021, ISSN (P) 2394-1588

International Advanced Research Journal in Science, Engineering and Technology

Impact Factor 8.311 ⁜ Peer-reviewed & Refereed journal ⁜ Vol. 13, Issue 1, January 2026

DOI: 10.17148/IARJSET.2026.13143

Sustainable Water Purification: Iron Filings for Dye Adsorption

Moamen O. Ali[1], Saddam A. Alaskary [1], Wafaa M. Hosny[1], Mamdouh A. Gadalla[2], Mai H. Roushdy[1]

Chemical Engineering Department, The British University in Egypt, El-Shorouk City 11837, Cairo, Egypt[1]

Chemical Engineering Department, Port Said University, 42526 Port Fouad, Egypt[2]

Abstract: This research explores the potential of iron filings as a sustainable adsorbent for the removal of synthetic dyes from wastewater, with a focus on Methyl Orange and Methylene Blue, two dyes commonly used in industrial processes. The iron filings were comprehensively characterized through chemical analysis, mineralogical assessment, particle size distribution, scanning electron microscopy (SEM), and Fourier transform infrared (FTIR) spectroscopy to evaluate their adsorption properties. The effects of key operational parameters—including adsorbent dosage, initial dye concentration, and contact time—on removal efficiency were systematically investigated, with experimental data analyzed using Design Expert software. Findings show that iron filings exhibit high adsorption capacity toward Methyl Orange, with FTIR analysis confirming the functional groups responsible for the adsorption mechanism. Adsorption isotherm and kinetic modeling indicated that Methyl Orange removal is consistent with Langmuir and Freundlich isotherms and follows both pseudo-first- and pseudo-second-order kinetics, while Methylene Blue removal aligns primarily with pseudo-first-order kinetics. Overall, the study highlights iron filings as an efficient, cost-effective, and environmentally sustainable material for dye removal in wastewater treatment applications.

Keywords: Iron filings, Methyl Orange (MO), Methylene Blue (MB), FTIR, SEM, RSM, adsorption isotherms, kinetics, wastewater treatment.

I. INTRODUCTION

The dyeing industry is one of the largest consumers of water, generating effluents rich in chemicals and coloring compounds that require proper treatment before discharge into natural water bodies. However, treating dyehouse wastewater remains a major challenge due to its complex and highly variable composition [1]. Methylene Blue (MB) is among the most widely used dyes in the textile sector, particularly for dyeing and finishing, yet excessive exposure poses risks to humans and aquatic ecosystems, including skin irritation, neurological disorders, and cardiovascular complications [2], [3]. Methyl Orange (MO), another common dye found in industrial effluents, is an anionic, watersoluble azo dye produced from sulfanilic acid and sodium nitrate. It is frequently employed in dyeing processes and is associated with high biochemical oxygen demand (BOD), chemical oxygen demand (COD), and suspended solids, all of which negatively affect aquatic life [2], [4].

Over the past century, multiple technologies have been developed to treat wastewater, with extensive research exploring various methods and materials to achieve efficient contaminant removal [5]. Conventional techniques include coagulation, flocculation, flotation or sedimentation, filtration, and adsorption, all of which are applied at different stages of treatment to reduce general pollutants and toxic substances [6]. Recent advancements emphasize integrating physical, chemical, and biological processes to improve treatment performance while supporting sustainability. These innovations are increasingly vital given the rising global demand for freshwater and the pressures of water scarcity caused by population growth [7].

Several methods have been investigated for dye removal from wastewater, including ion exchange, biodegradation, oxidation, membrane processes, adsorption, and solvent extraction [8], [9]. Each technique presents limitations: ion exchange is costly, membrane filtration suffers from low flow rates, and biodegradation is often slow and nutrientdependent. Among these, adsorption has emerged as one of the most attractive methods, owing to its simplicity, affordability, rapid operation, and minimal infrastructure requirements [10]. Iron filings, a byproduct of metalworking industries, have recently gained attention as an effective adsorbent material. Their abundance, low cost, and ease of application make them a practical candidate for dye removal, offering a sustainable solution to MO and MB contamination challenges [11].

This study investigates the adsorption behavior of iron filings for the removal of MO and MB dyes, focusing on optimizing operational parameters such as contact time, pH, initial dye concentration, and adsorbent dosage. In addition, the work examines the mechanisms underlying the adsorption process to better understand dye–adsorbent interactions.

IARJSET ISSN (O) 2393-8021, ISSN (P) 2394-1588

International Advanced Research Journal in Science, Engineering and Technology

Impact Factor 8.311 ⁜ Peer-reviewed & Refereed journal ⁜ Vol. 13, Issue 1, January 2026

DOI: 10.17148/IARJSET.2026.13143

By demonstrating the potential of repurposed industrial waste as a treatment medium, this research supports the advancement of sustainable water purification strategies and highlights iron filings as a viable material for practical applications in dye-polluted environments [11].

II. METHODOLOGY FOR RESEARCH

A. Raw Material

Iron filings, a solid waste byproduct of metalworking industries, were collected from a steel facility in Egypt and evaluated as a sustainable and low-cost material for the treatment of dye-contaminated water. The following points summarize their suitability:

Abundance and Cost-Effectiveness:

Iron filings are widely available and inexpensive, making them highly suitable for large-scale water treatment applications. Their use also supports the recycling of industrial waste, thereby contributing to environmental sustainability [12].

Adsorption Mechanism:

The adsorption of dye molecules onto iron filings occurs through both physical and chemisorption pathways. Their relatively high surface area enhances the overall adsorption capacity [13].

Factors Affecting Adsorption:

Key operational parameters—such as surface chemistry, pH, initial dye concentration, temperature, contact time, and adsorbent dosage—directly influence the efficiency of dye removal. Optimization of these factors can significantly improve the adsorption performance of iron filings [14].

Advantages:

Iron filings are environmentally benign and do not produce hazardous sludge. Their abundant supply and ease of handling promote their practical use in wastewater treatment. Moreover, they are capable of adsorbing both monolayers and multilayers of dye molecules [15].

Challenges:

Despite their potential, challenges remain regarding the regeneration and reuse of iron filings, as well as overcoming certain operational limitations in large-scale treatment systems [16].

Summary:

Overall, iron filings present a promising and sustainable alternative for dye removal, aligning with global efforts toward achieving cleaner and more efficient water resources.

B. Assessment of Solid Waste

The solid waste was subjected to a series of analytical techniques to evaluate its composition and structural characteristics:

Chemical Analysis (XRF):

X-ray fluorescence spectrometry (XRFS) was employed to determine the elemental composition of the waste by measuring secondary X-radiation emitted from the sample after excitation with an X-ray source. This method quantified the concentration of oxides in accordance with ASTM guidelines (C114-18) [17].

Mineralogical Analysis (XRD):

X-ray diffraction (XRD) was conducted to identify crystalline phases rather than elemental composition. Phase identification was performed using a PANalytical certified program and the International Center of Diffraction Database

IARJSET ISSN (O) 2393-8021, ISSN (P) 2394-1588

International Advanced Research Journal in Science, Engineering and Technology

Impact Factor 8.311 ⁜ Peer-reviewed & Refereed journal ⁜ Vol. 13, Issue 1, January 2026

DOI: 10.17148/IARJSET.2026.13143

(ICDD). Copper was used as the anode material, with continuous scanning under operating conditions of 30 mA and 40 kV [18].

Particle Size Distribution (PSD):

The particle size distribution was assessed using screen analysis, based on standard sieves with specified openings, in compliance with ASTM D422-2007 [19] and ASTM E11-2009 [20].

Scanning Electron Microscopy (SEM):

SEM was utilized to study the surface morphology and structural changes of the adsorbent both before and after dye adsorption. Prior to adsorption, SEM imaging revealed the surface features of the material—such as pores, cracks, and irregularities—that influence adsorption efficiency, as well as particle aggregation affecting surface area. After adsorption, SEM micrographs confirmed dye attachment, showing changes including pore blockage, swelling, or surface deformation. These insights validated the adsorption performance of the solid waste and provided visual evidence of dye removal.

Fourier Transform Infrared Spectroscopy (FTIR):

FTIR spectroscopy was applied to obtain the infrared spectra of the material in both solid and treated states. This technique records high-resolution spectral data across a wide range simultaneously, offering a clear advantage over dispersive spectrometers that measure narrower wavelength ranges [21].

C. Dye Removal Experiment

Preparation of Dye Solutions (MB or MO) with Different Concentrations:

A stock solution of each dye (100 mg/L) was prepared in a 1 L volumetric flask:

a) 0.1 g of dye powder was dissolved in a small volume of distilled water and transferred into a 1000 mL volumetric flask.

The solution was then diluted to the mark with distilled water.

b) The resulting 100 mg/L stock solution was further diluted to obtain the required concentrations using the dilution equation:

$$C_i \times V_i = C_f \times V_f$$

c) Test solutions with the desired concentrations were prepared accordingly.

Addition of Adsorbent:

The prepared dye solutions were treated by adding the required mass of iron filings (solid waste adsorbent).

Adsorption Procedure:

Adsorption experiments were conducted at varying time intervals, with the solutions agitated on a shaker at 300 rpm.

Filtration Step:

After adsorption, the mixtures were centrifuged at 3000 rpm for 10 minutes, and the supernatant was collected in clean, dry flasks for further analysis.

Analysis and Calculations:

a) The residual dye concentration in each sample was determined by measuring absorbance at the maximum wavelength (λmax): 464 nm for Methyl Orange and 664 nm for Methylene Blue, using a spectrophotometer.

b) Concentrations were calculated using the calibration curve equation: $y=ax$

IARJSET ISSN (O) 2393-8021, ISSN (P) 2394-1588

International Advanced Research Journal in Science, Engineering and Technology

Impact Factor 8.311 ⁜ Peer-reviewed & Refereed journal ⁜ Vol. 13, Issue 1, January 2026

DOI: 10.17148/IARJSET.2026.13143

where absorbance (y) divided by the constant (a) yields the unknown dye concentration (x) after adsorption.

D. Experimental Design

Response Surface Methodology (RSM) was employed to design the experimental framework, with detailed analysis performed using Design-Expert version 13 software [22]. The primary response variable was dye removal efficiency, while the independent factors—contact time, adsorbent dosage, and initial dye concentration—were designated as variables A, B, and C, respectively. The factor ranges are summarized in Table 1.

TABLE I FACTOR AFFECTING THE DYE REMOVAL PROCESS

Factor	**Label**	**Ranges**	
		Minimum	**Maximum**
Contact time (min)	A	1	4
Amount of Adsorbent (gm in 80 ml)	B	0.2	1.4
Initial Dye Concentration (mg/l)	C	0.2	3

To ensure efficiency and reliability in the experimental program, the design of runs was established using an uncertainty matrix approach, which reduces the total number of required experiments while preserving statistical robustness. This strategy allows for the systematic evaluation of key variables and their interactions without excessive experimental effort. The sequence of runs was randomized to eliminate bias and minimize potential errors associated with uncontrolled factors. Following each run, dye removal efficiency was determined and used as the primary response variable for subsequent modeling and optimization. The complete experimental matrix, outlining the combinations of process parameters investigated, is shown in Table 2.

TABLE II EXPERIMENTAL RUNS MATRIX FOR THE USED ADSORBENT

Run	**A**	**B**	**C**
1	10	0.2	0.2
2	150	0.2	0.2
3	10	1.4	0.2
4	150	1.4	0.2
5	10	0.2	3.0
6	150	0.2	3.0
7	10	1.4	3.0
8	150	1.4	3.0
9	38	0.8	1.6
10	198	0.8	1.6
11	80	0.2	1.6
12	80	1.8	1.6
13	80	0.8	0.8
14	80	0.8	4.0
15	80	0.8	1.6

Numerical optimization of the experimental variables was conducted to achieve defined objectives, focusing on both economic and environmental considerations. The optimization strategy aimed to minimize treatment costs while maximizing dye removal efficiency. The procedures incorporated regression analysis, graphical interpretation, and numerical optimization, all performed using Design-Expert version 13 (Stat-Ease Inc., Minneapolis, MN, USA) [22].

IARJSET ISSN (O) 2393-8021, ISSN (P) 2394-1588

International Advanced Research Journal in Science, Engineering and Technology

Impact Factor 8.311 ⁜ Peer-reviewed & Refereed journal ⁜ Vol. 13, Issue 1, January 2026

DOI: 10.17148/IARJSET.2026.13143

III. RESULTS AND DISCUSSION

The second objective of this study was to assess the potential of iron filings solid waste as an adsorbent for the removal of Methylene Blue (MB) and Methyl Orange (MO). This section presents the characterization results, which confirm the suitability of the material for adsorption applications.

A. Iron Filings Solid Waste Characterization:

a) Chemical Analysis:

The chemical composition of the iron filings is shown in Table 3. The waste primarily consists of Fe_2O_3 (96.15%), with only trace amounts of SiO_2, CaO, MnO, and other oxides. A minor loss on ignition (0.7%) is attributed to CO_2 release during heating. The high Fe_2O_3 content indicates that the material is a strong candidate for dye adsorption, consistent with findings reported in earlier studies.

TABLE III CHEMICAL ANALYSIS OF SOLID WASTE

Oxide	**Percentage, %**
Fe2O3	96.15
SiO2	1.25
CaO	0.91
MnO	0.49
TiO2	0.07
Na2O	0.04
P2O5	0.04
MgO	0.01
Al2O3	□0.01
K2O	□0.01
Cl	□0.01
SO3	□0.01
Loss on Ignition	0.7

b) Mineralogical Analysis:

X-ray diffraction (XRD) analysis, as shown in Fig. 1, identified hematite (α-Fe_2O_3) as the predominant crystalline phase, present in a rhombohedral structure, as shown in Fig. 2. Two reference codes were observed: JCPDS-00-024-0072 and JCPDS-00-033-0664, corresponding to hematite and burnt ochre hematite, respectively. Minor phases of quartz and calcite were also detected. These results are in good agreement with the XRF analysis, confirming hematite as the main phase and supporting its potential as an adsorbent.

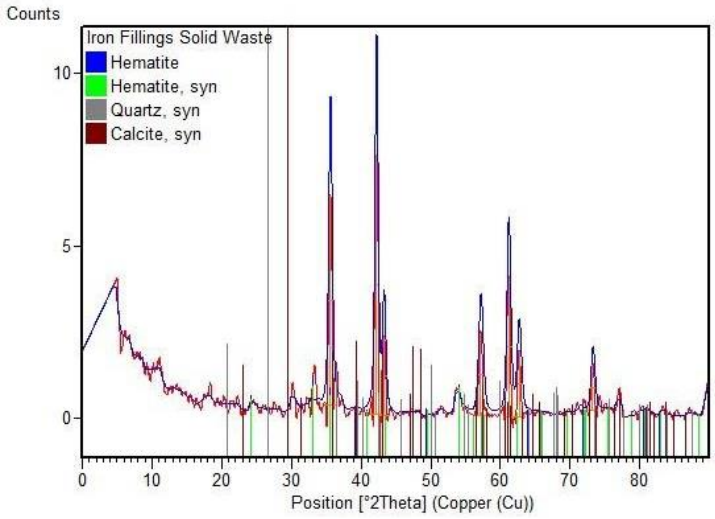

Fig. 1 Mineralogical analysis of Iron Fillings Solid Waste

IARJSET ISSN (O) 2393-8021, ISSN (P) 2394-1588

International Advanced Research Journal in Science, Engineering and Technology

Impact Factor 8.311 ⁜ Peer-reviewed & Refereed journal ⁜ Vol. 13, Issue 1, January 2026

DOI: 10.17148/IARJSET.2026.13143

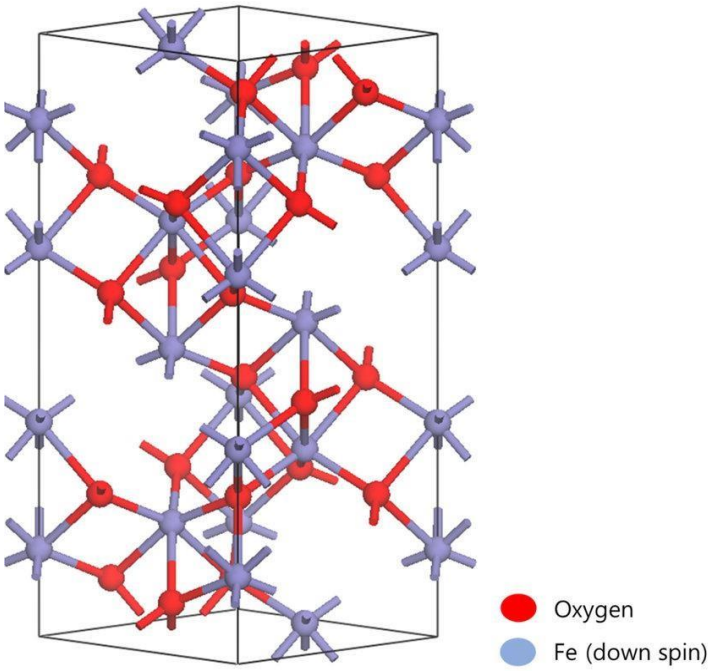

Fig. 2 Hematite (□-Fe2O3) with rhombohedral structure

Screen Analysis:

The particle size distribution, measured using a Malvern device, indicated an average size of 549.9 nm, as shown in Fig. 3. The fine particle size suggests a relatively high surface area, which enhances adsorption activity.

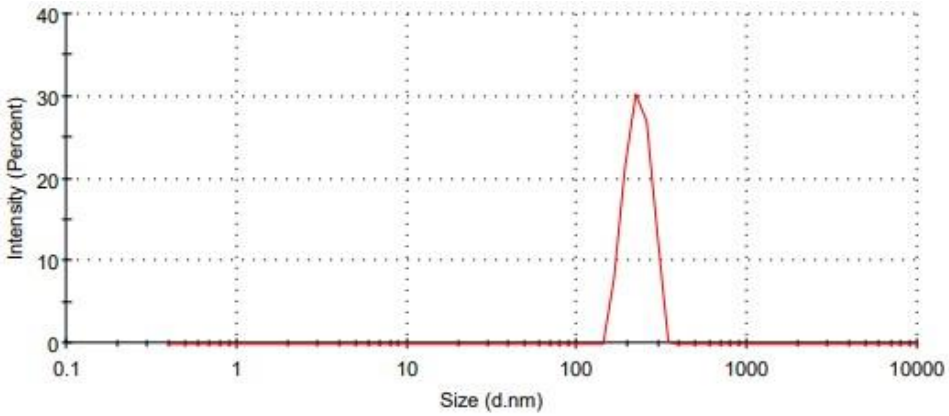

Fig. 3 Cumulative screen analysis curve of EAFD waste

d) SEM Analysis:

Scanning Electron Microscopy revealed a heterogeneous surface morphology with irregular shapes, pores, and active centers, as shown in Fig. 4. Such structural features are favorable for adsorption, confirming that the material possesses a surface well-suited for dye uptake.

IARJSET ISSN (O) 2393-8021, ISSN (P) 2394-1588

International Advanced Research Journal in Science, Engineering and Technology

Impact Factor 8.311 ⁜ Peer-reviewed & Refereed journal ⁜ Vol. 13, Issue 1, January 2026

DOI: 10.17148/IARJSET.2026.13143

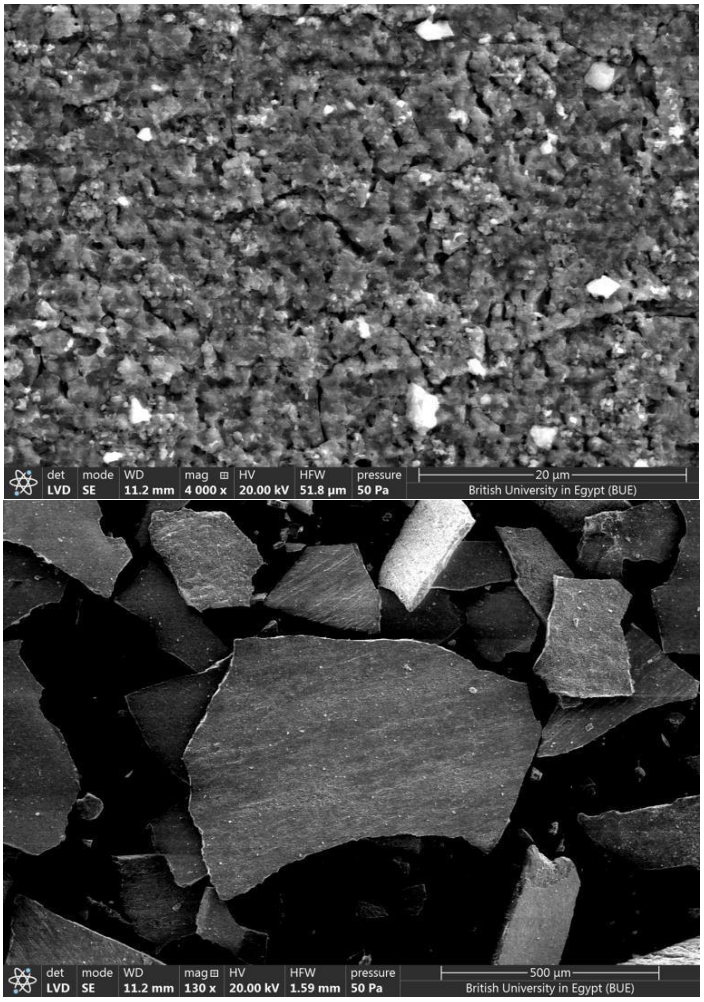

Fig. 4 SEM figures of Solid Waste

B. Process Modelling Using Design-Expert:

The dye removal efficiency was determined for each experimental run, and models were developed using Design-Expert version 13 to describe the relationship between process parameters and removal performance. Analysis of Variance (ANOVA) was conducted at a 95% confidence level to evaluate the significance of the models using *p*- and *F*-values, where the *p*-value indicates the probability that the observed results occurred by chance (with values < 0.05 generally considered significant), and the *F*-value reflects the ratio of model variance to residual variance, with higher values signifying a stronger model fit. The optimal model for Methylene Blue (MB) was identified as a reduced quadratic equation, while for Methyl Orange (MO), a linear model was found most suitable. Terms with p-values greater than 0.1 were excluded to simplify the models. The final reduced models are expressed in Eq. (1) and Eq. (2):

$$\boldsymbol{X = 8.448 + 0.089\,A + 81.735\,B + 11.398\,C - 11.227\,BC - 22.578\,B^2} \quad (1)$$

$$\boldsymbol{Y = 39.842 + 0.0825\,A + 11.058\,B + 6.498\,C} \quad (2)$$

where X represents MB removal efficiency and Y represents MO removal efficiency; A = contact time, B = adsorbent dosage, and C = initial dye concentration.

The ANOVA results for MB and MO are summarized as shown in Table 4 and Table 5. The predicted values exhibited strong agreement with the experimental results, as shown in Fig. 5 and Fig. 6, confirming the adequacy of the models.

IARJSET ISSN (O) 2393-8021, ISSN (P) 2394-1588

International Advanced Research Journal in Science, Engineering and Technology

Impact Factor 8.311 ⁜ Peer-reviewed & Refereed journal ⁜ Vol. 13, Issue 1, January 2026

DOI: 10.17148/IARJSET.2026.13143

TABLE IV RESULTS OF ANOVA FOR REDUCED QUADRATIC MODEL FOR MB DYE REMOVAL RESPONSE

Source	Sum of Squares	df	Mean Square	F-value	p-value	
Model	4346.79	5	869.36	7.79	0.0011	significant
A-Contact Time	435.81	1	435.81	3.91	0.0681	
B-Amount of Adsorbent	2921.45	1	2921.45	26.19	0.0002	
C-Initial Dye Concentration	126.92	1	126.92	1.14	0.3041	
BC	711.45	1	711.45	6.38	0.0242	
B^2	590.22	1	590.22	5.29	0.0373	
R^2	0.8357					

TABLE V RESULTS OF ANOVA FOR LINEAR MODEL FOR MO DYE REMOVAL RESPONSE

Source	Sum of Squares	df	Mean Square	F-value	p-value	
Model	1798.12	3	599.37	12.73	0.0002	significant
A-Contact Time	371.68	1	371.68	7.89	0.0126	
B-Amount of Adsorbent	518.28	1	518.28	11.01	0.0044	
C-Initial Dye Concentration	921.63	1	921.63	19.57	0.0004	
	0.8047					

The correlation between predicted and experimental dye removal efficiencies for MB and MO is illustrated as shown in Fig. 5 and Fig. 6.

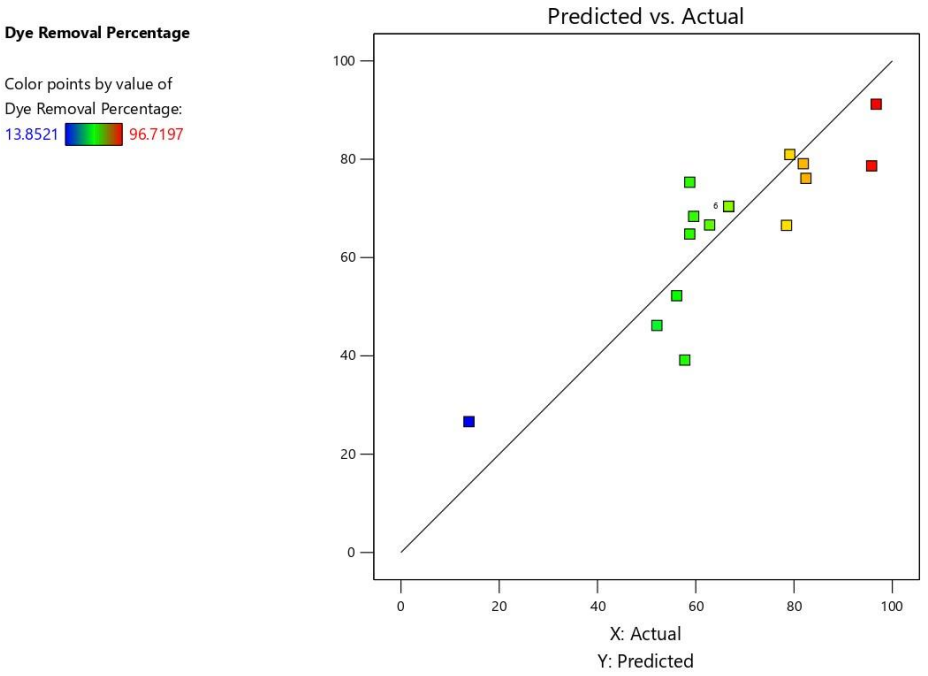

Fig. 5 The link between the predicted and experimental MB dye removal efficiency

IARJSET ISSN (O) 2393-8021, ISSN (P) 2394-1588

International Advanced Research Journal in Science, Engineering and Technology

Impact Factor 8.311 ⁜ Peer-reviewed & Refereed journal ⁜ Vol. 13, Issue 1, January 2026

DOI: 10.17148/IARJSET.2026.13143

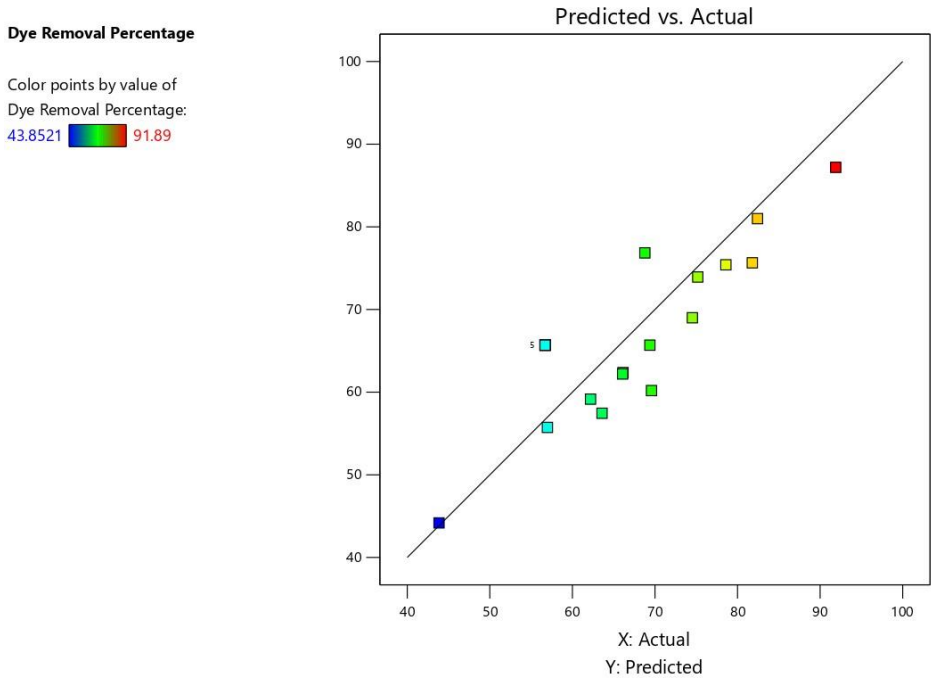

Fig. 6 The link between the predicted and experimental MO dye removal efficiency

a) Variation of Dye Removal Percentage with Process Conditions

The influence of individual process parameters on dye removal efficiency is illustrated as shown in Fig. 7 and Fig. 8. Increasing initial dye concentration enhanced removal efficiency due to a higher driving force, which reduced mass transfer resistance. Similarly, longer contact times improved removal up to a steady state, where equilibrium was reached. Increasing adsorbent dosage further improved separation by providing more active adsorption sites.

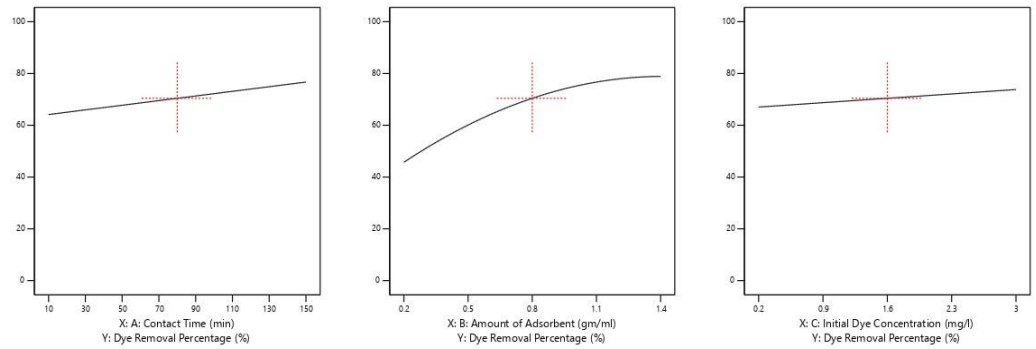

Fig. 7 The impact of all process parameters on MB dye removal %

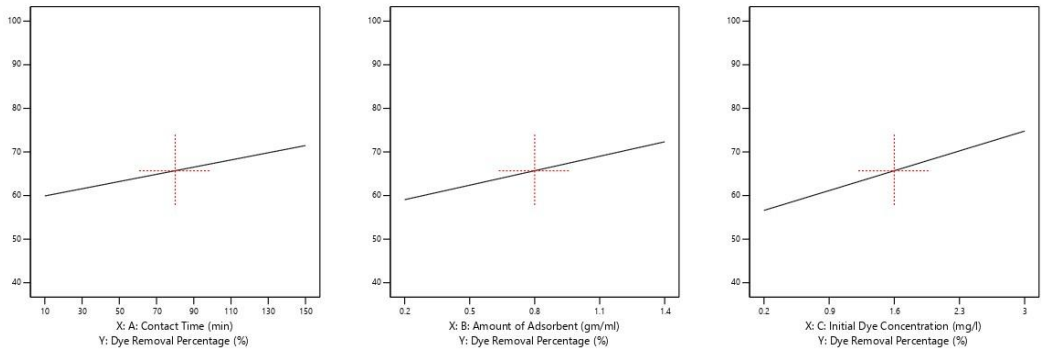

Fig. 8 The impact of of all process parameters on MO dye removal %

IARJSET ISSN (O) 2393-8021, ISSN (P) 2394-1588

International Advanced Research Journal in Science, Engineering and Technology

Impact Factor 8.311 ⁜ Peer-reviewed & Refereed journal ⁜ Vol. 13, Issue 1, January 2026

DOI: 10.17148/IARJSET.2026.13143

b) Interaction of Process Parameters

The combined effects of process variables on dye removal are shown as contour and 3D plots. For MB, the interactions between contact time and adsorbent dosage, as well as between adsorbent dosage and dye concentration, are illustrated in Fig. 9 through Fig. 12. For MO, the interactions between adsorbent dosage and contact time are depicted in Fig. 13 and Fig. 14. These plots highlight the interdependence of variables and their collective impact on removal performance.

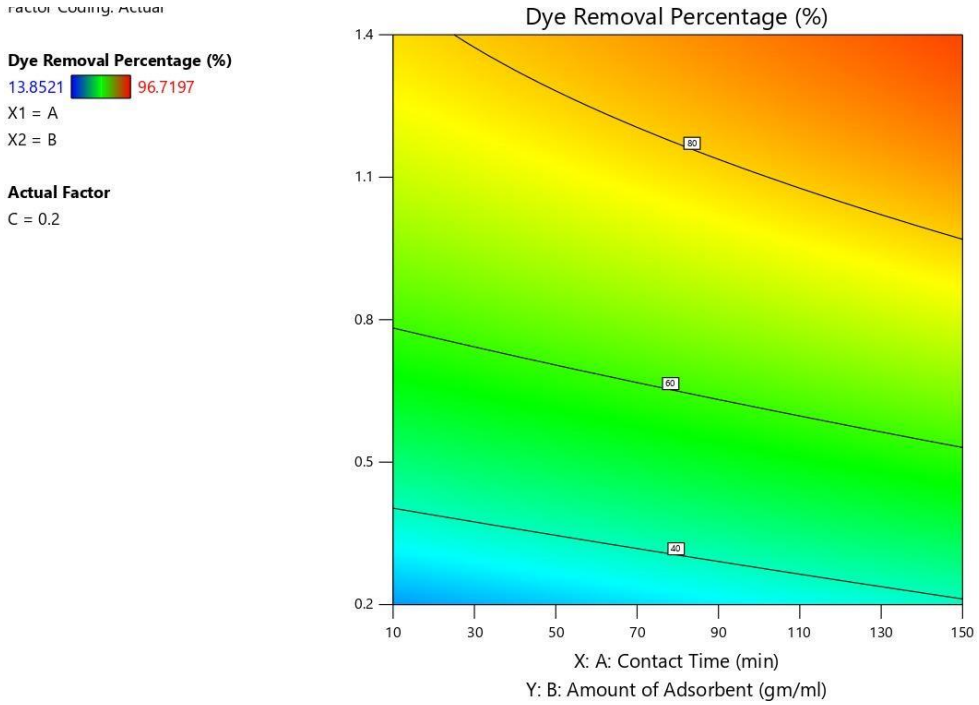

Fig. 9 The link between MB removal efficiency, contact time, and adsorbent amount interactions as a contour plot

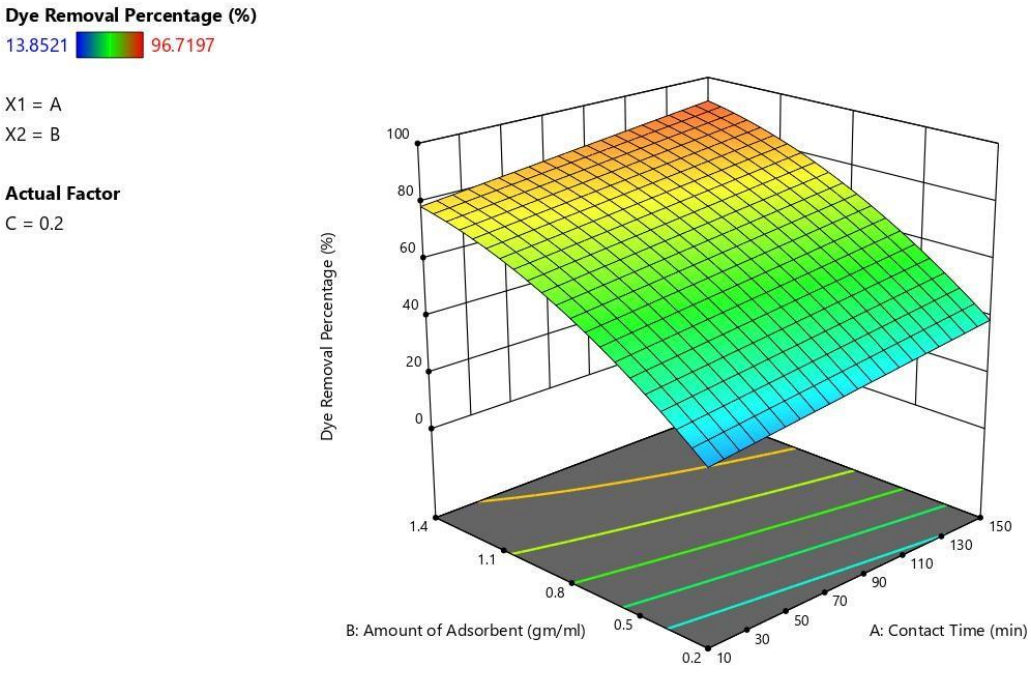

Fig. 10 The link between MB removal efficiency, contact time, and adsorbent amount interactions as a 3D plot

IARJSET ISSN (O) 2393-8021, ISSN (P) 2394-1588

International Advanced Research Journal in Science, Engineering and Technology

Impact Factor 8.311 ⁜ Peer-reviewed & Refereed journal ⁜ Vol. 13, Issue 1, January 2026

DOI: 10.17148/IARJSET.2026.13143

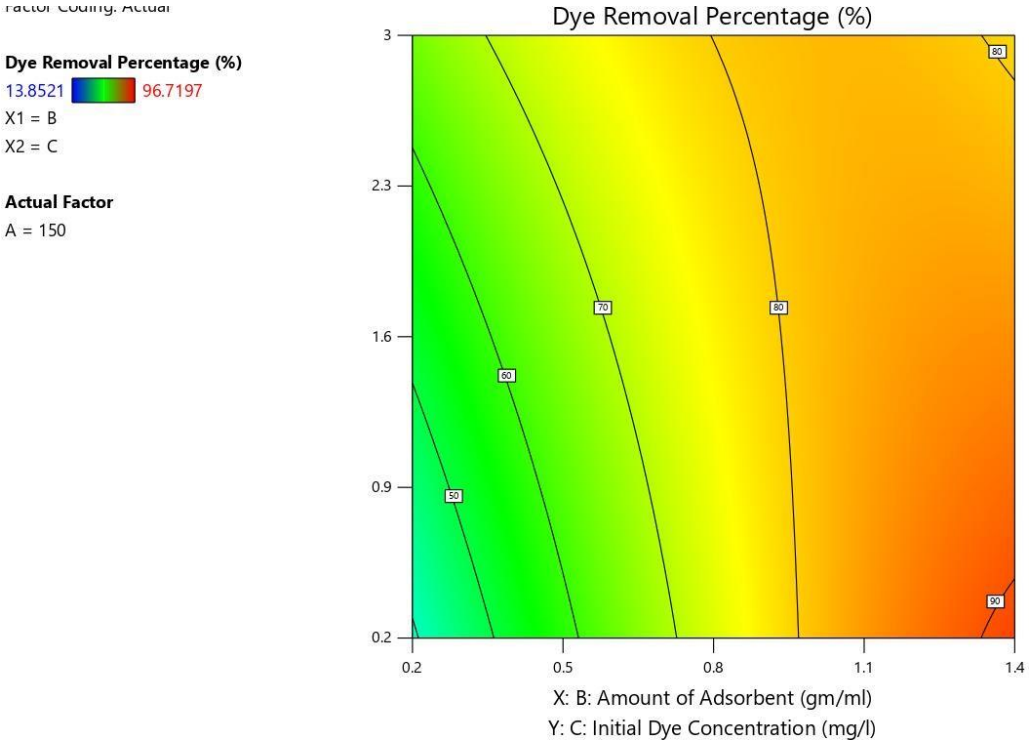

Fig. 11 The link between the MB dye removal, adsorbent amount, and initial dye concentration interactions as a contour plot

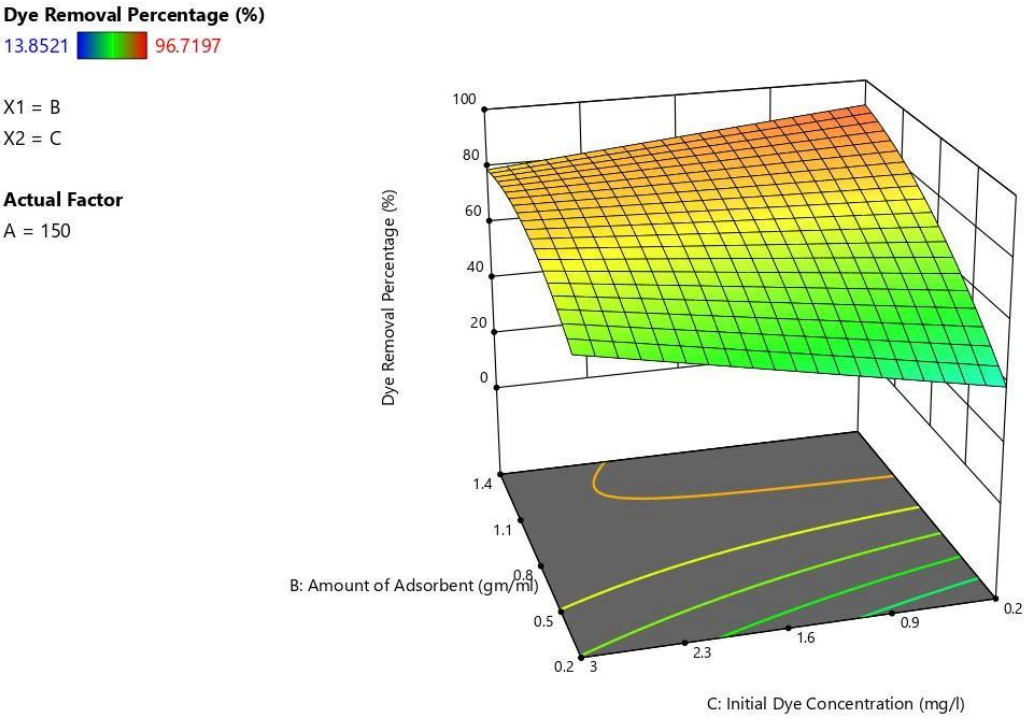

Fig. 12 The link between the MB dye removal, adsorbent amount, and initial dye concentration interactions as a 3D plot.

IARJSET ISSN (O) 2393-8021, ISSN (P) 2394-1588

International Advanced Research Journal in Science, Engineering and Technology

Impact Factor 8.311 ⁜ Peer-reviewed & Refereed journal ⁜ Vol. 13, Issue 1, January 2026

DOI: 10.17148/IARJSET.2026.13143

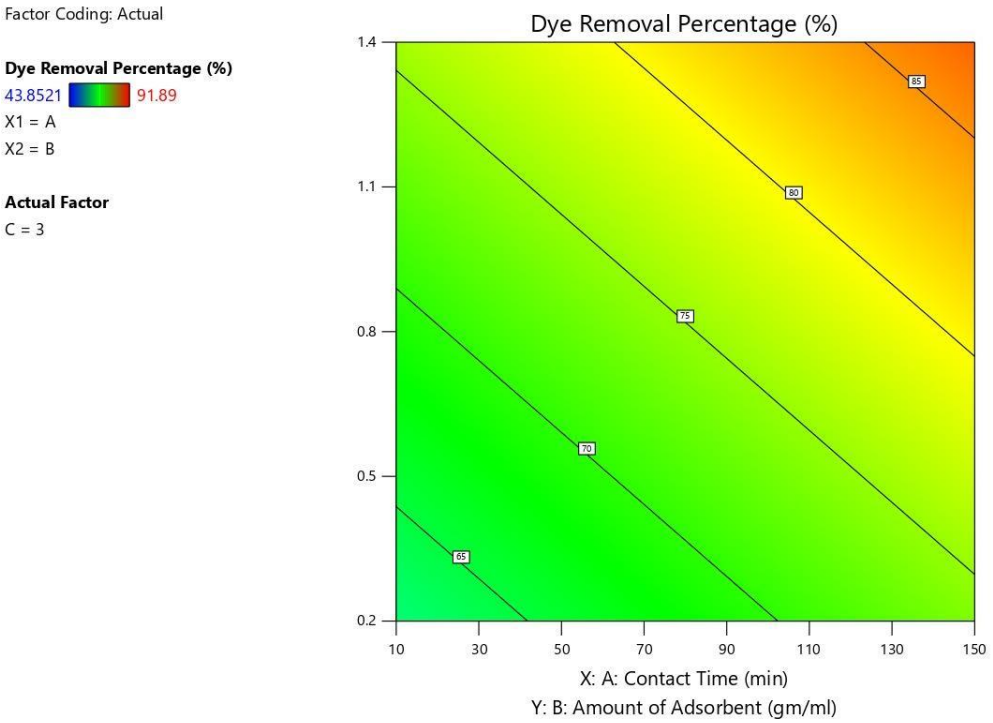

Fig. 13 The link between the MO dye removal, adsorbent amount, and contact time interactions as a contour plot

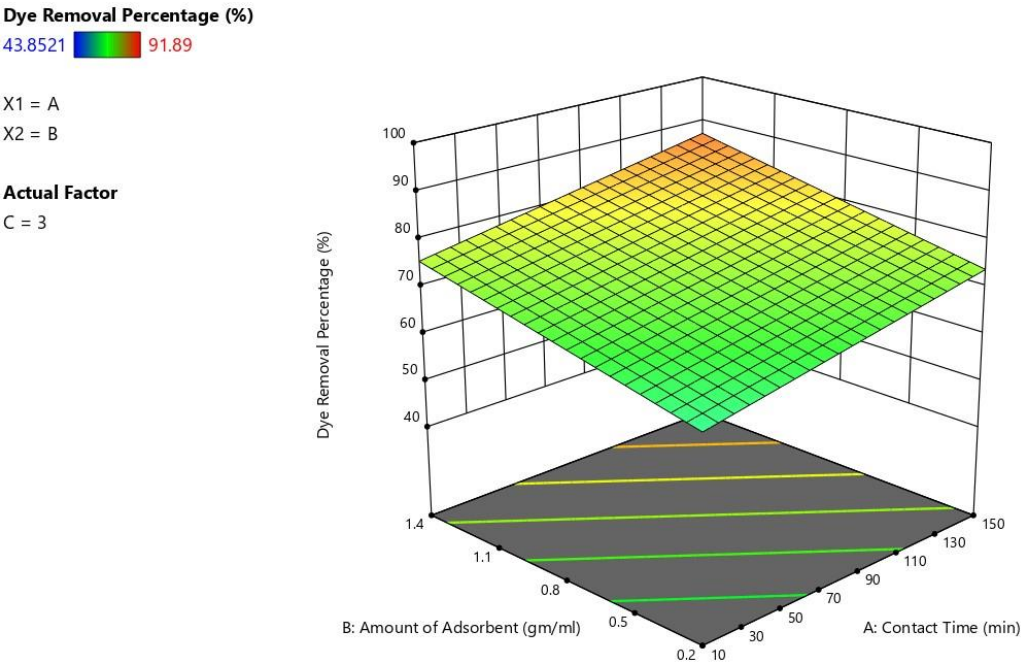

Fig. 14 The link between the MO dye removal, adsorbent amount, and contact time interactions as a 3D plot.

c) Process Optimization

Numerical optimization was performed using Design-Expert software to identify the optimal values of the independent variables (contact time, adsorbent dosage, and initial dye concentration) for maximizing dye removal. The desirability function was applied to balance economic and environmental objectives. Optimization goals and results are summarized as shown in Table 6.

IARJSET ISSN (O) 2393-8021, ISSN (P) 2394-1588

International Advanced Research Journal in Science, Engineering and Technology

Impact Factor 8.311 ⁜ Peer-reviewed & Refereed journal ⁜ Vol. 13, Issue 1, January 2026

DOI: 10.17148/IARJSET.2026.13143

TABLE VI OPTIMIZATION GOALS AND RESULTS

Name	Goal	Result for MB	Result for MO
A: Contact Time	minimize	10 min	10 min
B: Amount of Adsorbent	is in range	1.064 gm/ml	1.4 gm/ml
C: Initial Dye Concentration	Maximize	3 mg/l	3 mg/l
Dye Removal Percentage	Maximize	81.64%	81%

C. FTIR Analysis of Solid Waste Before and After Water Treatment:

The Fourier-transform infrared (FTIR) spectra were used to evaluate changes in the functional groups of the solid waste before and after dye adsorption. The comparative results are summarized as shown in Table 7, while the spectra for MB and MO adsorption are illustrated as shown in Fig. 15 and Fig. 16, respectively.

The data reveal notable differences between the FTIR spectra before and after adsorption in the case of MO, where several new peaks appeared and shifts in existing peaks were observed. These spectral changes indicate the involvement of chemisorption, suggesting strong interactions between MO molecules and the active sites of the adsorbent surface. In contrast, the spectra obtained after MB adsorption show minimal differences compared to the untreated solid waste, which implies that MB removal occurred primarily through physical adsorption rather than chemical bonding.

These observations provide preliminary evidence of the adsorption mechanisms and will be further validated through the analysis of adsorption isotherms and kinetic models.

TABLE VII CHANGES APPEARED FTIR PEAKS BEFORE AND AFTER ADSORPTION

Solid Waste			Solid Waste + MB			Solid Waste + MO		
Peak No	X	Y	Peak No	X	Y	Peak No	X	Y
Peak 1	410.7905	0.94652	Peak 1	410.7905	0.94652	Peak 1	409.8262	0.94192
Peak 2	429.1122	0.96104	Peak 2	429.1122	0.96104	Peak 2	418.5049	0.94309
Peak 3	460.934	0.9634	Peak 3	460.934	0.9634	Peak 3	427.1836	0.94292
Peak 4	478.2913	0.98103	Peak 4	478.2913	0.98103	Peak 4	459.9697	0.95452
Peak 5	874.6173	0.98726	Peak 5	874.6173	0.98726	Peak 5	479.2556	0.97574
						Peak 6	486.0057	0.97742
						Peak 7	494.6843	0.98246
						Peak 8	503.363	0.98451
						Peak 9	513.006	0.9853

IARJSET ISSN (O) 2393-8021, ISSN (P) 2394-1588

International Advanced Research Journal in Science, Engineering and Technology

Impact Factor 8.311 ⁜ Peer-reviewed & Refereed journal ⁜ Vol. 13, Issue 1, January 2026

DOI: 10.17148/IARJSET.2026.13143

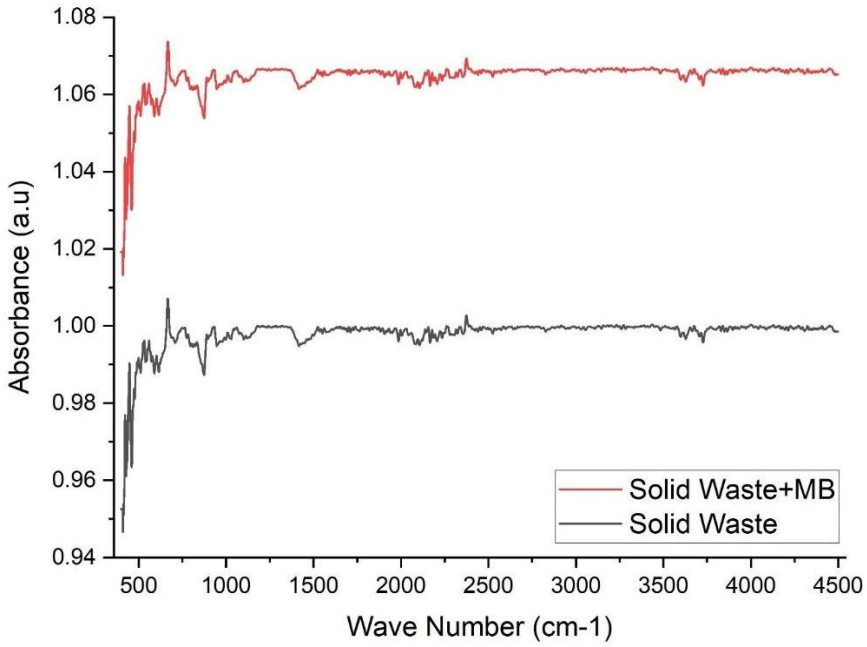

Fig. 15 FTIR figure for solid waste before and after adsorption process for MB

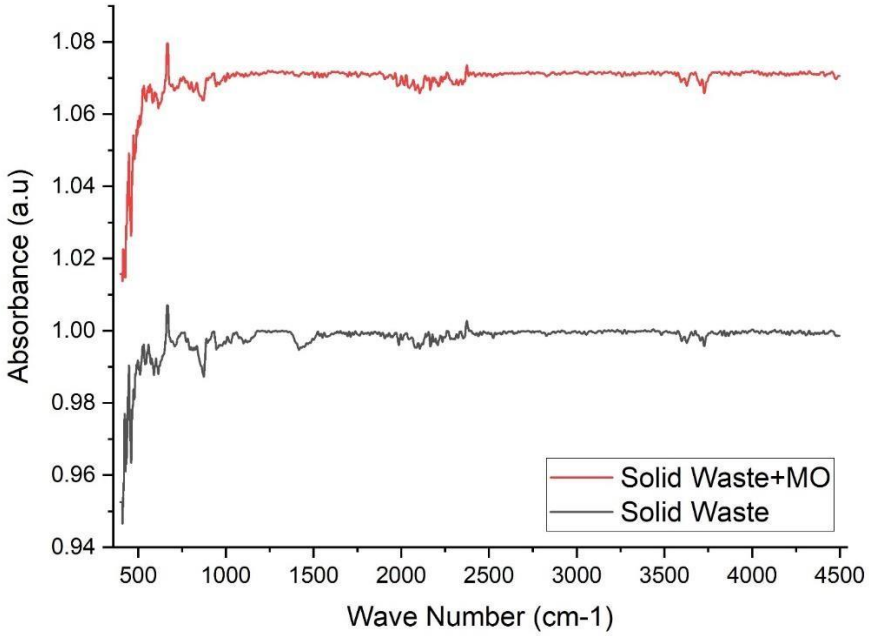

Fig. 16 FTIR figure for solid waste before and after adsorption process for MO

D. Adsorption and Kinetics Study for MO Removal:

a) Adsorption Isotherm Models

Adsorption isotherm analysis was performed to evaluate the maximum adsorption capacity of the solid waste and to describe the relationship between the equilibrium concentration of MO in solution and the amount adsorbed on the solid phase. Isotherm models provide insights into how dye molecules distribute between liquid and solid phases once equilibrium is reached, which is crucial for optimizing adsorption system design. Four widely used isotherm models—Langmuir, Freundlich, Dubinin–Radushkevich, and Halsey—were applied in their linearized forms to the equilibrium

IARJSET ISSN (O) 2393-8021, ISSN (P) 2394-1588

International Advanced Research Journal in Science, Engineering and Technology

Impact Factor 8.311 ⁜ Peer-reviewed & Refereed journal ⁜ Vol. 13, Issue 1, January 2026

DOI: 10.17148/IARJSET.2026.13143

data to identify the most suitable model. All isotherm experiments were carried out at pH = 8 and a contact time of 80 minutes.

Langmuir Isotherm:

The Langmuir model assumes monolayer adsorption on a homogeneous surface and is expressed as:

$$1/qe = 1/Q0 + (1/(K*Q0)) * (1/Ce)$$

Where q_e is the equilibrium adsorption capacity (mg/g), C_e is the equilibrium concentration (mg/L), Q° is the maximum monolayer capacity, and K is the Langmuir constant. The separation factor R_l is defined as:

$$RL = 1 / (1 + K*Co)$$

The Langmuir plot, as shown in Fig. 17, yielded a correlation coefficient (R^2) of 0.9627, indicating excellent model fit. Positive slope and intercept values confirm the suitability of the model. The separation factor R_l fell between 0 and 1, verifying favorable adsorption. Key results are summarized as shown in Table 8.

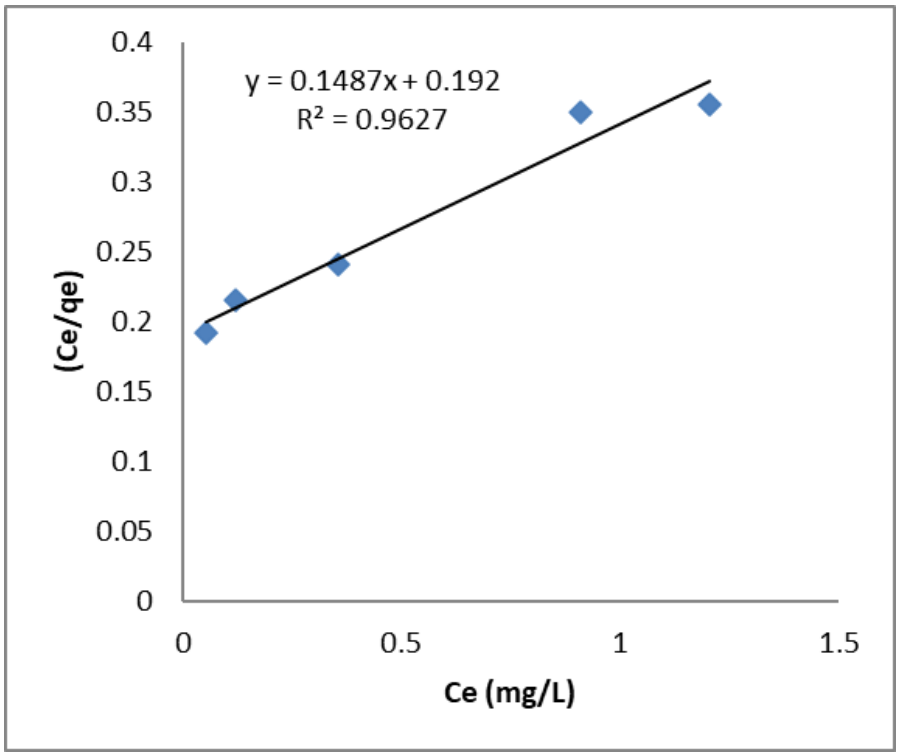

Fig. 17 Langmuir Fit

TABLE VIII RESULTS OF LANGMUIR MODEL FIT

Maximum monolayer adsorption capacity	**qmax (mg/g)**	**6.725**
Langmuir constant which indicates the adsorption energy	K (L/mg)	0.774479167

IARJSET ISSN (O) 2393-8021, ISSN (P) 2394-1588

International Advanced Research Journal in Science, Engineering and Technology

Impact Factor 8.311 ⁜ Peer-reviewed & Refereed journal ⁜ Vol. 13, Issue 1, January 2026

DOI: 10.17148/IARJSET.2026.13143

Indicates the types of isotherms are favorable if (0<RL<1), linear (RL=1) or unfavorable (RL=0)	RL (separation factor)	0.089720884

Freundlich Isotherm:

The Freundlich model assumes heterogeneous surface adsorption and multilayer formation, expressed as:

$$\log(qe) = \log(KF) + (1/n) * \log(Ce)$$

Where K_F is the adsorption capacity and 1/n represents adsorption intensity. As shown in Fig. 18, the correlation coefficient ($R^2 = 0.7892$) was relatively low, indicating poor fit to the data. This suggests that adsorption did not occur on a heterogeneous surface but instead followed monolayer adsorption, consistent with Langmuir behaviour.

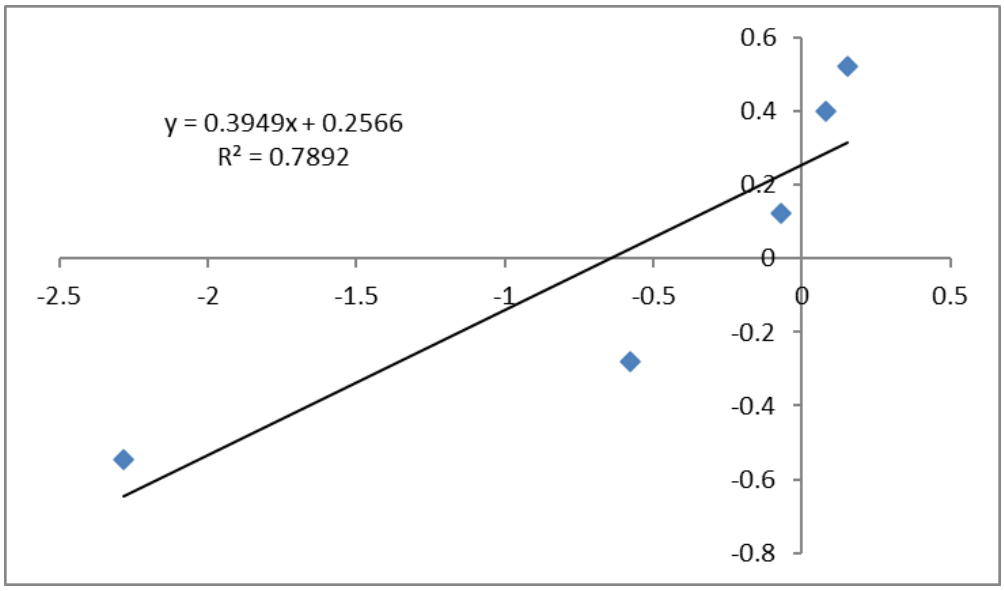

Fig. 18 Freundlich Fit

Halsey Isotherm:

The Halsey model, expressed as:

$$\ln(qe) = (1/n) * \ln(K) - (1/n) * \ln(Ce)$$

Where K and n are Halsey isotherm constant and they can be obtained from the slope and intercept of the plot of ln qe versus ln Ce. Was also tested. As shown in Fig. 19, the model produced an R^2 value of 0.7892, confirming a weak fit similar to Freundlich. This further supports that adsorption of MO followed the Langmuir model.

IARJSET ISSN (O) 2393-8021, ISSN (P) 2394-1588

International Advanced Research Journal in Science, Engineering and Technology

Impact Factor 8.311 ⁜ Peer-reviewed & Refereed journal ⁜ Vol. 13, Issue 1, January 2026

DOI: 10.17148/IARJSET.2026.13143

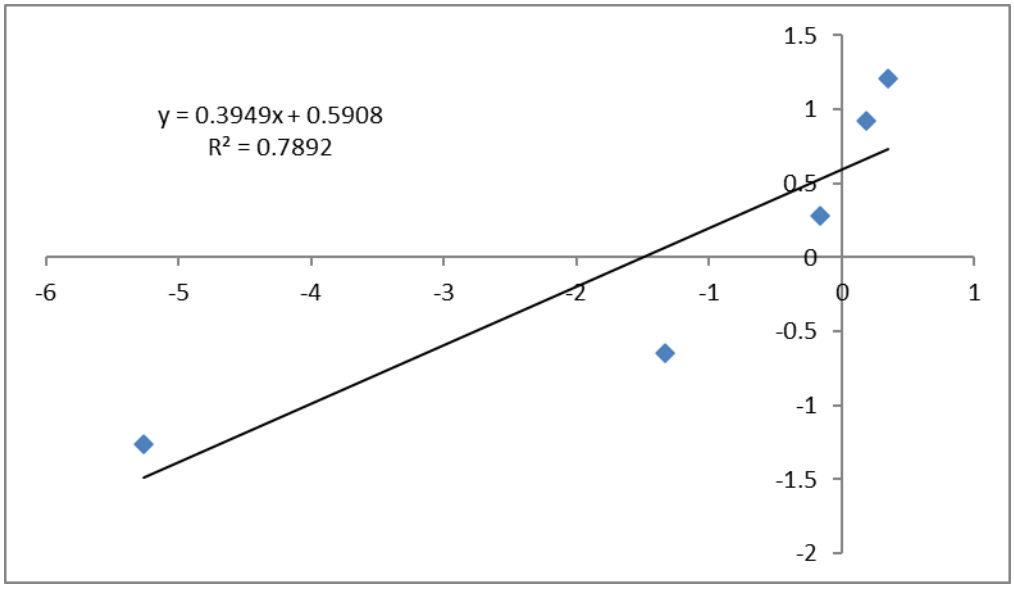

Fig. 19 Halsey Fit

Dubinin–Radushkevich (D–R) Isotherm

The D–R model, which helps distinguish between physical and chemical adsorption, is expressed as:

$$\ln(qe) = \ln(qmax) - B*R^2*T^2 * [\ln(1 + 1/Ce)]^2$$

Where qmax is maximum adsorption capacity, B is the D–R constant, R is the universal gas constant, T is temperature, and E is mean adsorption energy (E = 1 / sqrt{2B}). Results are summarized as shown in Table 9, and the corresponding fit is shown in Fig. 20. The calculated mean adsorption energy (E = 16.5 kJ/mol) exceeded 16 kJ/mol, suggesting chemisorption as the dominant mechanism.

TABLE IX RESULTS OF DUBININ-RADUSHKEVICH MODEL FIT

slope (BR2T2)	0.0113
B (mol2/kJ2)	0.00183903
E (kJ/mol)	16.48885938
Intercept (ln qmax)	-1.2169
qmax (mg/g)	0.2961468

IARJSET ISSN (O) 2393-8021, ISSN (P) 2394-1588

International Advanced Research Journal in Science, Engineering and Technology

Impact Factor 8.311 ⁜ Peer-reviewed & Refereed journal ⁜ Vol. 13, Issue 1, January 2026

DOI: 10.17148/IARJSET.2026.13143

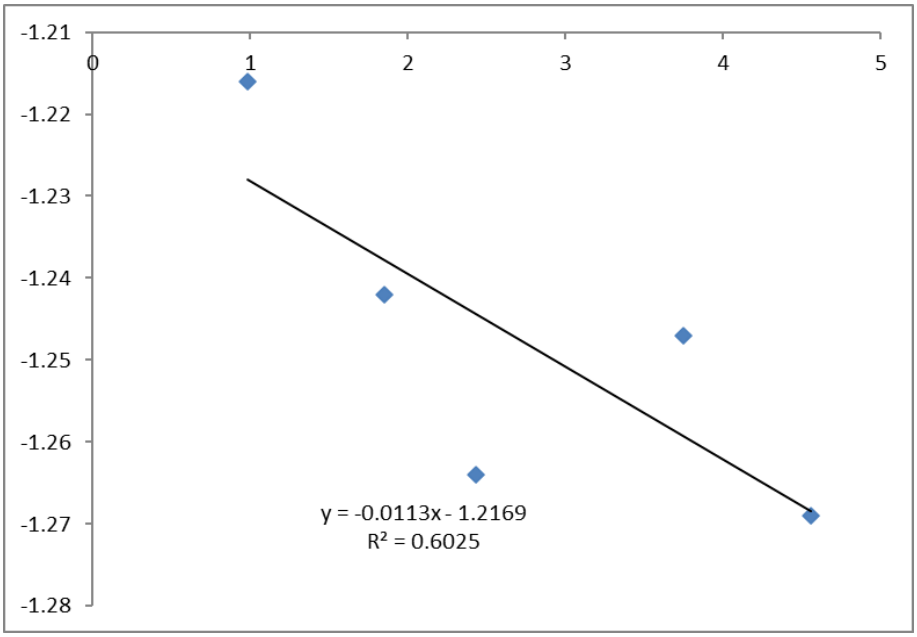

Fig. 20 Dubinin-Radushkevich Fit

b) Adsorption Kinetics Model for MO Removal

Pseudo First-Order Reaction Kinetics

The pseudo-first-order kinetic model is expressed as:

$$\ln(qe - qt) = -k1*t + \ln(qe)$$

Where qt is adsorption capacity at time t and k_1 is the rate constant. The fit, as shown in Fig. 21, yielded an R^2 of 0.7013. Calculated q_e values deviated significantly from experimental data, confirming that the model does not adequately describe the adsorption process. This result aligns with the dominance of chemisorption, where first-order kinetics are less applicable.

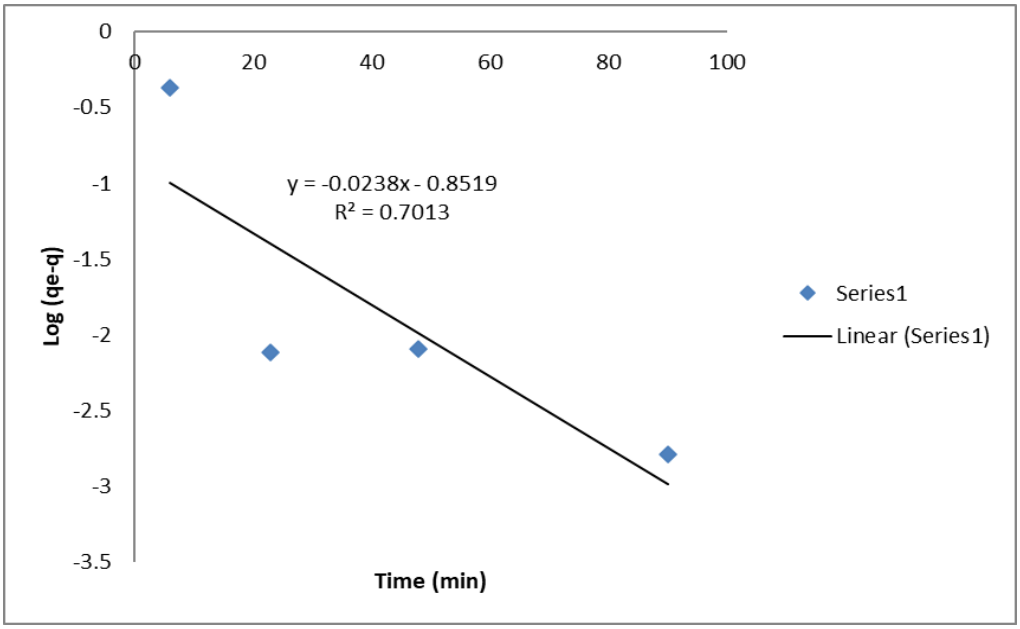

Fig. 21 Pseudo First-Order Reaction Kinetics Fit

IARJSET ISSN (O) 2393-8021, ISSN (P) 2394-1588

International Advanced Research Journal in Science, Engineering and Technology

Impact Factor 8.311 ⁜ Peer-reviewed & Refereed journal ⁜ Vol. 13, Issue 1, January 2026

DOI: 10.17148/IARJSET.2026.13143

Pseudo-Second-Order Kinetics

The pseudo-second-order kinetic model, suitable for chemisorption processes, is expressed as:

$$t/qt = 1/(k2*qe^2) + (t/qe)$$

Where k_2 is the rate constant of second-order adsorption. As shown in Fig. 22, the model provided an excellent fit (R^2 = 0.9836). The calculated and experimental q_e values were in close agreement, further confirming chemisorption as the governing mechanism. The rate constant was determined to be 0.005 mg/g·min.

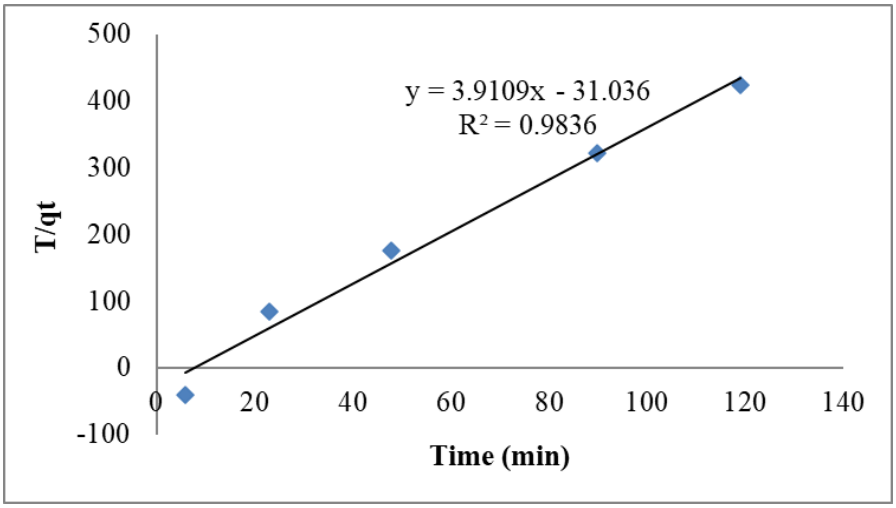

Fig. 22 Pseudo Second-Order Reaction Kinetics-Chemisorption Fit

E. Adsorption and Kinetics Study for MB Removal:

a) Adsorption Isotherm Models for MB Removal

Langmuir Isotherm:
The Langmuir model was first applied to the equilibrium data. As shown in Fig. 23, the model yielded a correlation coefficient (R^2 = 0.877). However, the regression equation exhibited a negative intercept, which deviates from the theoretical assumptions of the Langmuir model. This indicates that the experimental data do not adequately fit the Langmuir isotherm, and monolayer adsorption on a homogeneous surface cannot be assumed for MB.

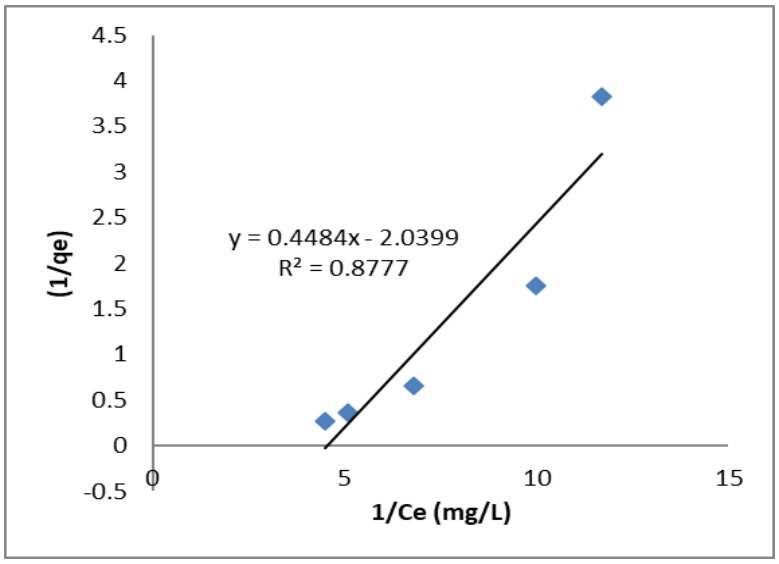

Fig. 23 Langmuir Fit

IARJSET ISSN (O) 2393-8021, ISSN (P) 2394-1588

International Advanced Research Journal in Science, Engineering and Technology

Impact Factor 8.311 ⁜ Peer-reviewed & Refereed journal ⁜ Vol. 13, Issue 1, January 2026

DOI: 10.17148/IARJSET.2026.13143

Freundlich Isotherm

The Freundlich model, which describes adsorption on heterogeneous surfaces with multilayer formation, was evaluated next. The fit, as shown in Fig. 24, produced a strong correlation ($R^2 = 0.9807$), confirming that this model accurately represents the adsorption process. This suggests that MB adsorption occurs through multilayer coverage, consistent with physical adsorption. The calculated parameters are summarized as shown in Table 10.

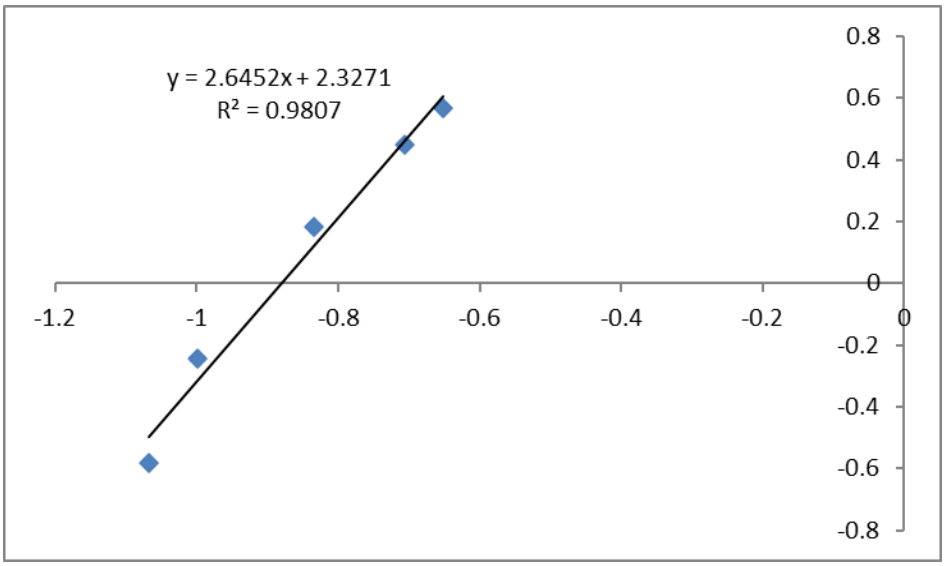

Fig. 24 Freundlich Fit

TABLE X FREUNDLICH RESULTS FIT

Adsorption intensity	1/n	2.5855
Freundlish constant which is in between 0 and 1	n	0.386772384
	log KF	2.3271
Freundlish constant which adsorption capacity	KF (L/mg)	212.3733413

Halsey Isotherm

The Halsey model was also applied, producing an identical R^2 value (0.9807) to the Freundlich model, as shown in Fig. 25. This further supports the conclusion that MB adsorption on the solid waste occurs in multilayers on a heterogeneous surface. Key parameters obtained from the model are summarized as shown in Table 11.

IARJSET ISSN (O) 2393-8021, ISSN (P) 2394-1588

International Advanced Research Journal in Science, Engineering and Technology

Impact Factor 8.311 ⁜ Peer-reviewed & Refereed journal ⁜ Vol. 13, Issue 1, January 2026

DOI: 10.17148/IARJSET.2026.13143

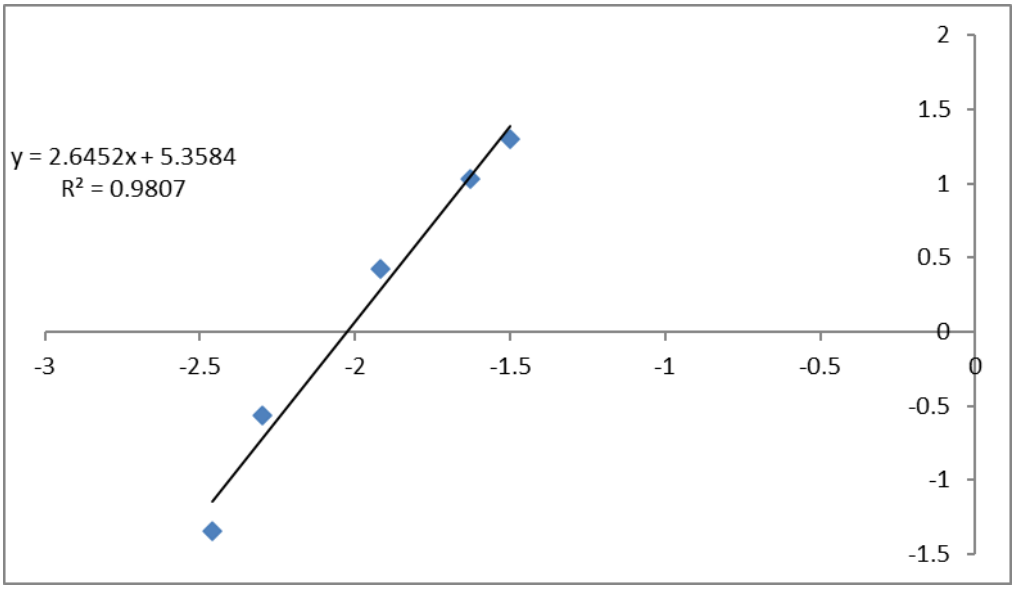

Fig. 25 Halsey Fit

TABLE XI HALSEY RESULTS FIT

slope (1/n)	2.6452
n	0.378043248
Intercept	5.3584
K	2.025706941

Dubinin–Radushkevich (D–R) Isotherm

The D–R model was also tested to assess the nature of adsorption. The results, as shown in Fig. 26 and summarized in Table 12, indicated a mean adsorption energy (E) of 1.43 kJ/mol. Since this value is below 8 kJ/mol, it confirms that MB adsorption is governed by a physical adsorption mechanism rather than chemisorption.

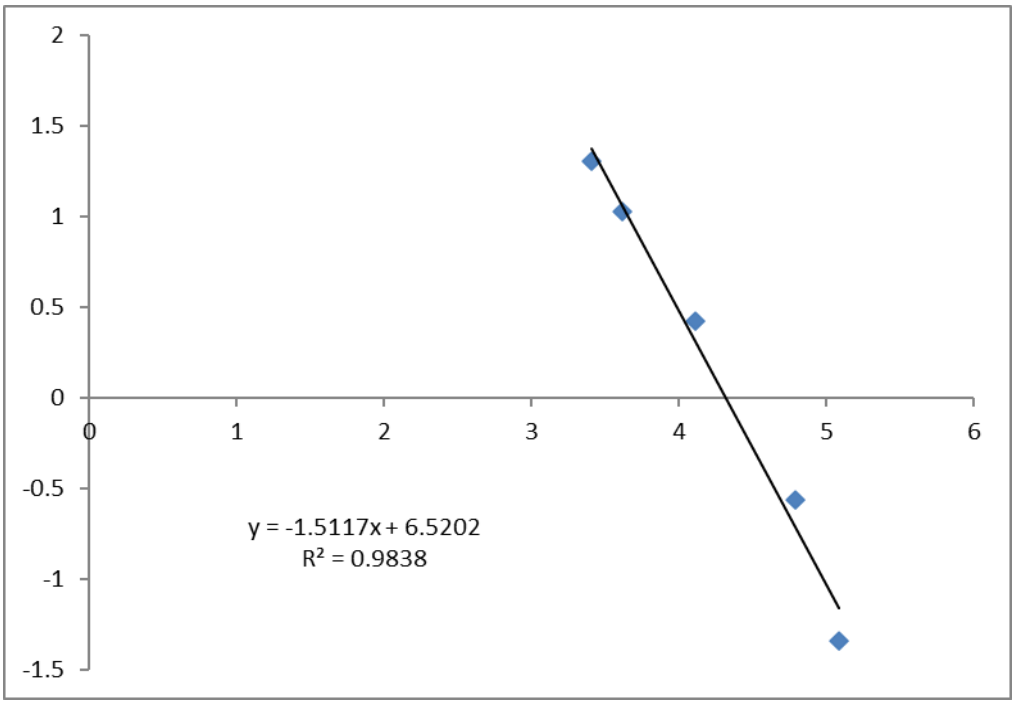

Fig. 26 Dubinin-Radushkevich Fit

IARJSET ISSN (O) 2393-8021, ISSN (P) 2394-1588

International Advanced Research Journal in Science, Engineering and Technology

Impact Factor 8.311 ⁜ Peer-reviewed & Refereed journal ⁜ Vol. 13, Issue 1, January 2026

DOI: 10.17148/IARJSET.2026.13143

TABLE XII DUBININ-RADUSHKEVICH RESULTS FIT

slope (BR2T2)	1.5117
B (mol2/kJ2)	0.246023133
E (kJ/mol)	1.425597843
Intercept (ln qmax)	6.5202
qmax (mg/g)	678.7141146

b) Adsorption Kinetics Models for MB Removal

Pseudo-First-Order Kinetics

The pseudo-first-order kinetic model was applied to the adsorption data, as shown in Fig. 27. The model demonstrated a strong fit (R^2 = 0.9584). Furthermore, the calculated equilibrium adsorption capacity (q_e) closely matched the experimental values, validating the suitability of this model. This finding is consistent with physical adsorption as the dominant mechanism for MB uptake. The rate constant was determined as 6×10^{-6} min^{-1}.

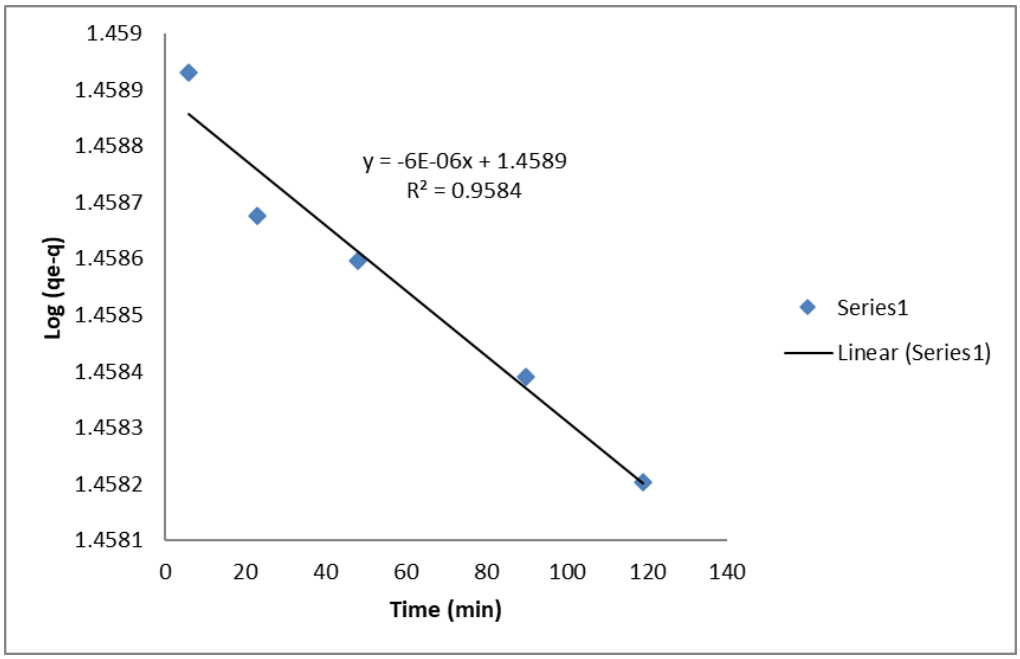

Fig. 27 Pseudo First-Order Reaction Kinetics fit

F. SEM Analysis Results:

The surface morphology of the adsorbent after the adsorption process was examined using Scanning Electron Microscopy (SEM). The images, as shown in Fig. 28, Fig. 29, and Fig. 30, reveal clear evidence of dye uptake. Compared to the untreated surface, which displayed open pores and active centers, the post-adsorption micrographs show that these active sites were covered by MB and MO molecules. The blockage of surface pores and reduction in visible active centers confirm that the dyes were successfully adsorbed onto the adsorbent surface, providing further validation of the adsorption efficiency observed in the isotherm and kinetic studies.

IARJSET ISSN (O) 2393-8021, ISSN (P) 2394-1588

International Advanced Research Journal in Science, Engineering and Technology

Impact Factor 8.311 ⁜ Peer-reviewed & Refereed journal ⁜ Vol. 13, Issue 1, January 2026

DOI: 10.17148/IARJSET.2026.13143

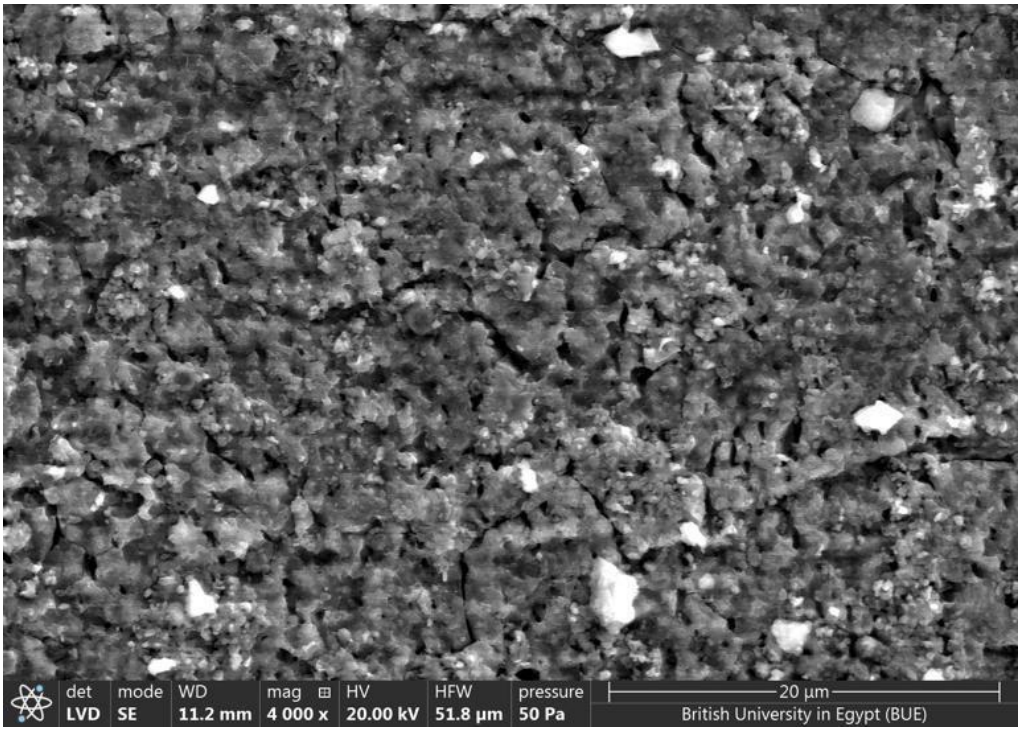

Fig. 28 SEM Analysis Result for Iron Filings before Adsorption Process

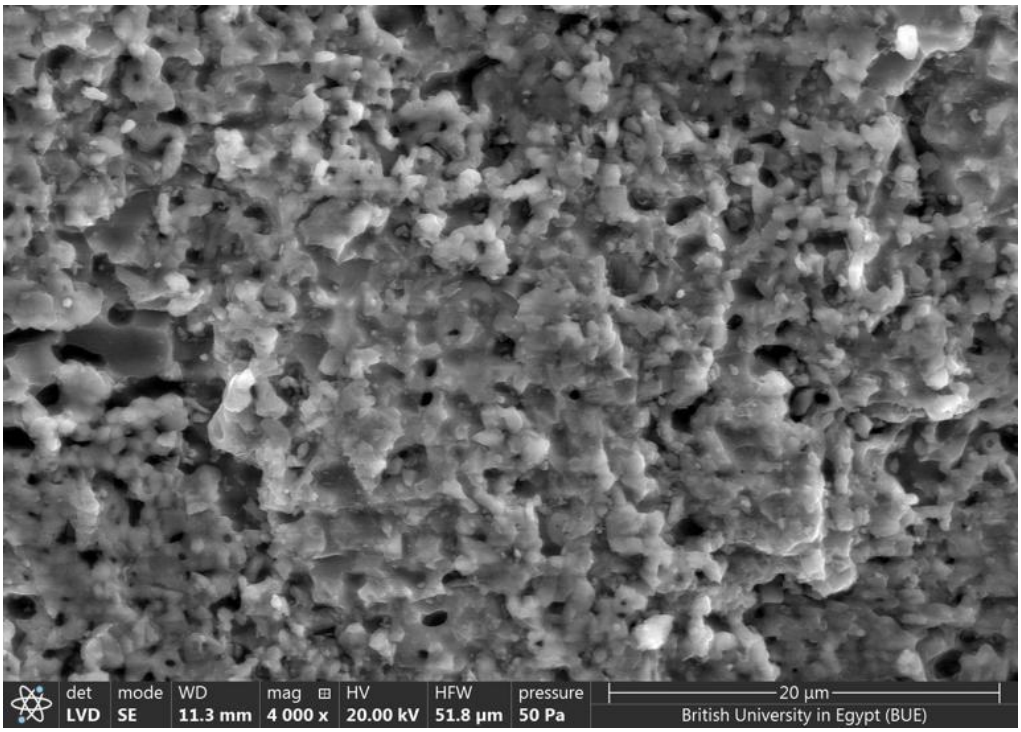

Fig. 29 SEM Analysis Result for Iron Filings after Adsorption process with MB

IARJSET ISSN (O) 2393-8021, ISSN (P) 2394-1588

International Advanced Research Journal in Science, Engineering and Technology

Impact Factor 8.311 ⁜ Peer-reviewed & Refereed journal ⁜ Vol. 13, Issue 1, January 2026

DOI: 10.17148/IARJSET.2026.13143

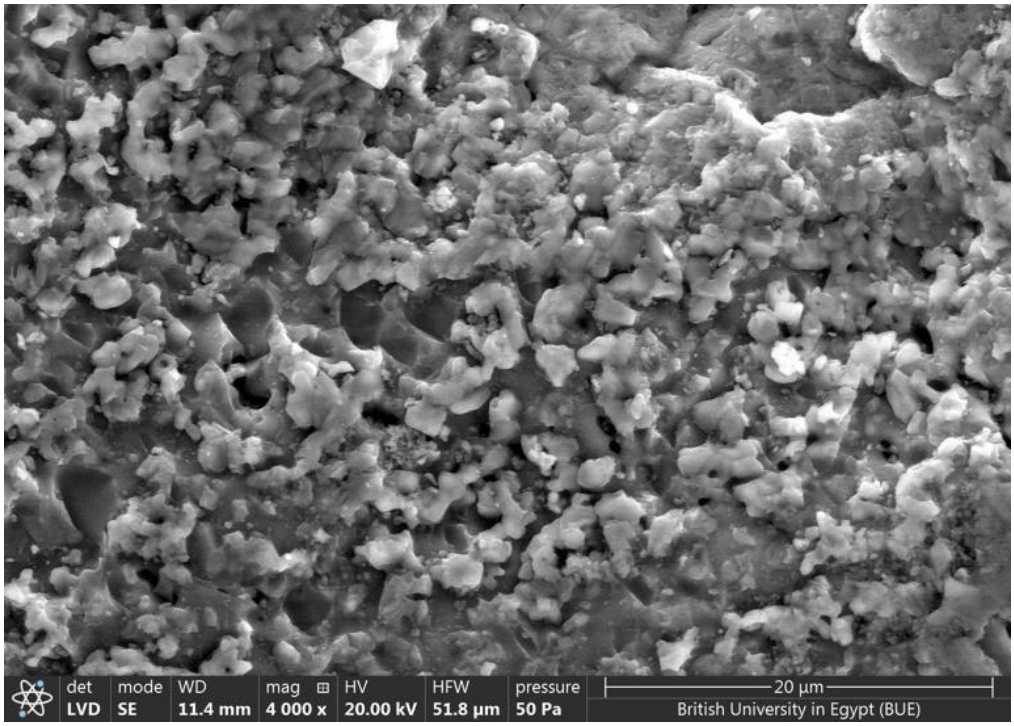

Fig. 30 SEM Analysis Result for Iron Filings after Adsorption process with MO

IV. CONCLUSION

This study demonstrated the potential of iron filings, an industrial byproduct, as an effective and sustainable adsorbent for the removal of Methyl Orange (MO) and Methylene Blue (MB) dyes from aqueous solutions. Comprehensive characterization using XRF, XRD, PSD, SEM, and FTIR confirmed that the material possesses favorable chemical and morphological properties for adsorption, with hematite (Fe_2O_3) as the dominant phase and surface features conducive to dye uptake.

The adsorption experiments revealed distinct behaviors for MO and MB. For MO, the Langmuir isotherm and pseudosecond-order kinetic model provided the best fit, indicating monolayer adsorption governed primarily by chemisorption. Conversely, MB adsorption was best described by the Freundlich and Halsey isotherms, alongside the pseudo-first-order kinetic model, suggesting multilayer adsorption dominated by physical interactions. FTIR and SEM analyses further supported these findings, showing chemical interaction in the case of MO and surface coverage consistent with physical adsorption for MB.

Optimization studies using Design-Expert software identified favorable process conditions, with contact time, adsorbent dosage, and dye concentration significantly influencing removal efficiency. Under optimized conditions, the maximum dye removal efficiencies achieved were 81.64% for MO and 81% for MB, underscoring the practical potential of iron filings as a low-cost and eco-friendly adsorbent.

Overall, this research highlights the dual environmental benefit of repurposing industrial waste while addressing dye pollution in wastewater. Iron filings offer a promising alternative for large-scale wastewater treatment, aligning with sustainable water management goals. Future work may focus on regeneration and reuse of the adsorbent to enhance operational feasibility and explore its applicability for a broader range of industrial contaminants.

REFERENCES

[1]. S. Sivamani and L. B. Grace, “Removal of Dyes from Wastewater using Adsorption-A Review,” 2009. [Online]. Available:
https://www.researchgate.net/publication/255966641 [2]. J. Rajendran, A. Panneerselvam, S. Ramasamy, and P. Palanisamy, “Methylene blue and methyl orange removal from wastewater by magnetic adsorbent based on activated carbon synthesised from watermelon shell,” *Desalination Water Treat*, vol. 317, Jan. 2024, doi: 10.1016/j.dwt.2024.100040. [3]. Ş. Parlayıcı and E. Pehlivan, “Biosorption of methylene blue and malachite green on biodegradable magnetic Cortaderia selloana flower spikes: modeling and equilibrium study,” *Int J Phytoremediation*, vol. 23, no. 1, pp. 26–40, 2021, doi: 10.1080/15226514.2020.1788502.

DOI: 10.17148/IARJSET.2026.13143

[4]. S. Rattanapan, J. Srikram, and P. Kongsune, "Adsorption of Methyl Orange on Coffee grounds Activated Carbon," in *Energy Procedia*, Elsevier Ltd, 2017, pp. 949–954. doi: 10.1016/j.egypro.2017.10.064.

[5]. M. M. H. Elzahar and M. Bassyouni, "Removal of direct dyes from wastewater using chitosan and polyacrylamide blends," *Sci Rep*, vol. 13, no. 1, Dec. 2023, doi: 10.1038/s41598-023-42960-y. [6]. M. M. Abou Alsoaud, M. A. Taher, A. M. Hamed, M. S. Elnouby, and A. M. Omer, "Reusable kaolin impregnated aminated chitosan composite beads for efficient removal of Congo red dye: isotherms, kinetics and thermodynamics studies," *Sci Rep*, vol. 12, no. 1, Dec. 2022, doi: 10.1038/s41598-022-17305-w.

[7]. F. Mushtaq *et al.*, "MnFe2O4/coal fly ash nanocomposite: a novel sunlight-active magnetic photocatalyst for dye degradation," *International Journal of Environmental Science and Technology*, vol. 17, no. 10, pp. 4233–4248, Oct. 2020, doi: 10.1007/s13762-020-02777-y.

[8]. M. Borges Mansur, "Resumo Extração por solventes aplicada à recuperação de metais e da água a partir de resíduos industriais e efluentes líquidos Solvent extraction for metal and water recovery from industrial wastes and effluents."

[9]. S. Selvakumar, R. Manivasagan, and K. Chinnappan, "Biodegradation and decolourization of textile dye wastewater using Ganoderma lucidum," *3 Biotech*, vol. 3, no. 1, pp. 71–79, Feb. 2013, doi: 10.1007/s13205-012-0073-5. [10]. S. Ho, "Removal of Dyes from Wastewater by Adsorption onto Activated Carbon: Mini Review," *Journal of Geoscience and Environment Protection*, vol. 08, no. 05, pp. 120–131, 2020, doi: 10.4236/gep.2020.85008.

[11]. M. Abid, M. Al-Tufaily, and Z. A. Hmoud, "USING OF WASTED FILINGS OF IRON TO ADSORB METHYLENE BLUE DYE FROM AQUEOUS SOLUTION," IJARET, 2014. [Online]. Available: www.iaeme.com/ijaret.asp

[12]. M. Dehghani, M. Nozari, A. Fakhraei Fard, M. Ansari Shiri, and N. Shamsedini, "Direct red 81 adsorption on iron filings from aqueous solutions; kinetic and isotherm studies," *Environmental Technology (United Kingdom)*, vol. 40, no. 13, pp. 1705–1713, Jun. 2019, doi: 10.1080/09593330.2018.1428228.

[13]. C. M. Ngwu, O. K. Amadi, M. O. Mac-Kalunta, and J. Onyeuwaoma, "SORPTION STUDIES ON THE REMOVAL OF NAPHTOL-AS DYE USING IRON FILINGS AS ADSORBENT," 2021.

[14]. A. Ahmad *et al.*, "Removal of Cationic Dyes by Iron Modified Silica/Polyurethane Composite: Kinetic, Isotherm and Thermodynamic Analyses, and Regeneration via Advanced Oxidation Process," *Polymers (Basel)*, vol. 14, no. 24, Dec. 2022, doi: 10.3390/polym14245416.

[15]. F. Barjasteh-Askari, M. Davoudi, M. Dolatabadi, and S. Ahmadzadeh, "Iron-modified activated carbon derived from agro-waste for enhanced dye removal from aqueous solutions," *Heliyon*, vol. 7, no. 6, Jun. 2021, doi: 10.1016/j.heliyon.2021.e07191.

[16]. N. R. J. Hynes *et al.*, "Modern enabling techniques and adsorbents based dye removal with sustainability concerns in textile industrial sector -A comprehensive review," *Journal of Cleaner Production*, vol. 272. Elsevier Ltd, Nov. 01, 2020. doi: 10.1016/j.jclepro.2020.122636.

[17]. ASTM C114-15, "Standard Test Methods for Chemical Analysis of Hydraulic Cement," *Annual Book of ASTM Standards*, vol. i, no. May, p. 32, 2018, doi: 10.1520/C0114-11A.

[18]. ASTM E2860-20 Standard Test Method for Residual Stress Measurement by X-Ray Diffraction for Bearing Steels, *Annual Book of ASTM Standards*. 2021. Accessed: Jun. 12, 2024. [Online]. Available: https://www.astm.org/e2860-20.html [19]. N. Engineering, "Particle Size Analysis - ASTM D422," no. 604597, pp. 70–138, 2017.

[20]. N. Sieve, "Standard Specification for Woven Wire Test Sieve Cloth and Test Sieves 1 E2427 Test Method for Acceptance by Performance Testing," pp. 1–11, 2017, doi: 10.1520/E0011-16.2.

[21]. M. A. Ganzoury, N. K. Allam, T. Nicolet, and C. All, "Introduction to Fourier Transform Infrared Spectrometry," *Renewable and Sustainable Energy Reviews*, vol. 50, pp. 1–8, 2015, doi: 10.1016/j.rser.2015.05.073.

[22]. D. C. Montgomery, Montgomery Design and Analysis of Experiments Eighth Edition. Arizona State University, vol. 2009, no. 2005. 2013.

